Spectroscopic Studies of Electrochemically Generated Cation Radical of Chlorophyll a in Organic Solvents

Rep. Fac. Sci., Kagoshima Univ.
No. 30, 17～25, 1997

Spectroscopic Studies of Electrochemically Generated Cation Radical of Chlorophyll a in Organic Solvents

Junichi KURAWAKI and Yoshihumi KUSUMOTO

(Received July 8, 1997)

Keywords : chlorophyll cation radical, electrolysis, spectroscopy, Raman spectra

Abstract

Spectroscopic studies of electrochemically generated cation radical of chlorophyll a (Chl) were carried out in various organic solvents. Absorption and resonance Raman (RR) spectra of Chl cation radical ($Chl^{+\cdot}$) exhibited remarkable spectral changes with oxidation. The major prominent changes of Raman bands observed upon oxidation of Chl are a large upshift of the C_9 keto-carbonyl stretching on ring V (C_9=O), downshifts of the coordination-state marker bands, and intensity and frequency changes of Raman bands in the C_aC_m and C_aN stretching modes. The large upshift of the C_9=O stretching mode indicates that there is a decrease in the conjugation between C_9=O and the macrocycle following one-electron oxidation. We could find some oxidation-state marker Raman bands in all organic solvents investigated in this study.

Introduction

The conformational changes of chlorophylls in photosystem (PS) I and photosystem (PS) II serve to control electron transfer by changing the interaction of the chromophore with the surrounding protein and altering the relative distances and orientations between donor and acceptor species (1, 2). As a result, a chlorophyll a (Chl) /Chl cation radical ($Chl^{+\cdot}$) radical pair is formed in the charge separation process in both PS I and PS II (3). Accordingly, it is important to investigate the structural and electronic properties of $Chl^{+\cdot}$ which influence the process of charge separation. Immense effort has been so far expended toward characterizing the spectroscopic properties of $Chl^{+\cdot}$ in addition to neutral Chl through absorption, magnetic resonance and vibrational spectroscopies (4-6). In spite of this effort, little information is available on the consequence of the precise structures for $Chl^{+\cdot}$. Resonance Raman (RR) spectroscopy is, however, a powerful tool for studying the molecular structures of the primary donor and cation and anion radicals produced by electron transfer. Only a few RR spectra of cation and anion radicals of Chl have been reported so far (6-8).

In this paper, therefore, we report spectroscopic results of electrochemically generated $Chl^{+\cdot}$ in various organic solvents by means of absorption, fluorescence and Raman spectroscopies. A purpose of our research is to elucidate the vibrational structures of $Chl^{+\cdot}$ and its models operating as the primary donor in PS I and PS II.

Experimental

Commercial Chl (Wako, > 95 %) was used as received and its purity was checked by measuring its absorption spectrum in ethanol. Prior to use, Chl was dried by repetitive codistillation from dichloromethane (CH_2Cl_2). All organic solvents

Department of Chemistry and BioScience, Faculty of Science, Kagoshima University, 21-35, Korimoto 1-chome, Kagoshima 890, Japan.

used in this work were spectroscopic grade or HPLC one, and were dried by vacuum distillation, and then stored over activated 3 Å molecular sieves. As a supporting electrolyte, tetrabutylammonium perchlorate (TBAP) was used. TBAP was purified by recrystallization from ethyl acetate and dried under vacuum at 100 ℃.

Absorption and fluorescence spectra of neutral Chl and $Chl^{+\cdot}$ were recorded on a Hitachi 228 spectrophotometer and a Hitachi 850 spectrofluorometer, respectively. Fluorescence lifetimes of $Chl^{+\cdot}$ were measured with a Horiba NAES-1100 time-resolved spectrophotometer equipped with a single-photon counting system. ESR spectra of $Chl^{+\cdot}$ were performed in an ESR spectrometer (JEOL JM-ME-3X). Raman spectra were recorded on a Jasco R-800 laser-Raman spectrophotometer under the conditions pre-resonating the Soret absorption band by using the 441.6 nm of a He-Cd laser (Kimmon Electric Co., Ltd., CD4601R). Experimental conditions were the same for all Raman experiments and are as follows: resolution 5 cm^{-1}; laser power <10 mW at the sample point. All measurements were conducted at 25 ℃.

Generation of $Chl^{+\cdot}$ and its spectroscopic measurements were performed in a home-made spectroelectrochemical cell (optical path length = 1 and 5 mm) containing a platinum mesh working electrode. Controlled-potential electrogeneration of $Chl^{+\cdot}$ was performed at the platinum electrode with a Hokuto Denko HA-301 potentiostat. The concentration of Chl in the sample solutions was adjusted between 1×10^{-4} and 5×10^{-4} M (1 M = 1 $moldm^{-3}$). The concentration of TBAP was kept at 0.1 M. In order to test the performance of this spectroelectrochemical cell used in this work, we measured representative absorption spectra of zinc tetraphenylporphyrin (ZnTPP) in CH_2Cl_2 during electrolysis at 0.8 V and ESR spectrum of the species produced at a final stage of electrolysis. The spectral behavior shown in Fig. 1 and g-value (2.002) obtained from ESR spectrum were very close to those reported by Fajer et al. (3); this result indicates that ZnTPP cation radical is produced via one-electron oxidation and this spectroelectrochemical cell can operate successfully.

Results and Discussion

Absorption spectroscopy of Chl and $Chl^{+\cdot}$

Absorption spectra of Chl are dominated by intense π-π^* transitions which occur in the visible

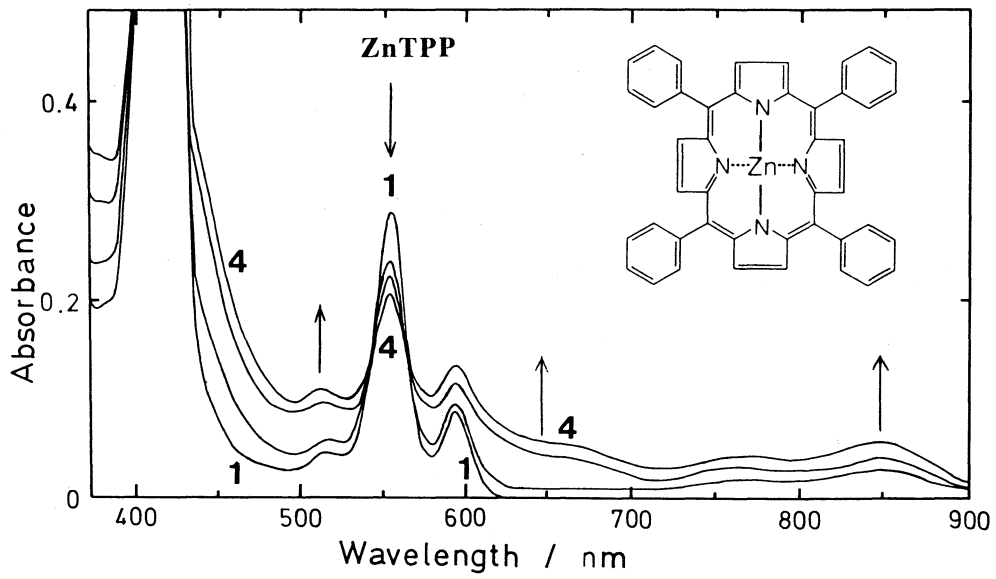

Fig. 1. Absorption spectral change of ZnTPP during electrolysis in dichloromethane (CH_2Cl_2). 1; absorption spectrum of neutral ZnTPP, 4; absorption spectrum of ZnTPP cation radical. Insert is molecular structure of ZnTPP.

region. Fig. 2 shows representative absorption spectra at various stages of electrolysis for three organic solvents. For example, the absorption spectrum of neutral Chl in CH_2Cl_2 solution shows maxima at 432 nm in the Soret region and at 666 nm in the red region (Fig. 2 (A)). The absorption peaks at 432 and 666 nm correspond to the B_x and Q_y transitions, respectively. Upon electrolysis at 0.85 V, the absorbance of these two bands gradually decreased and the Soret absorption maximum shifted from 432 to 415 nm. In addition, a new strong absorption bands at 415 nm and broad bands around 510, 700 and 815 nm appeared. As shown in Fig. 2 (A), the fact that well defined isosbestic points were observed at 426, 446, 609, 640 and 683 nm indicates the smooth course of this reaction. The ESR spectrum of the species produced at a final stage of electrolysis in CH_2Cl_2 solution (Fig. 2 (A), insert) showed only a single line at $g=2.004$; this species can be assigned to a π-cation radical of Chl ($Chl^{+\cdot}$).

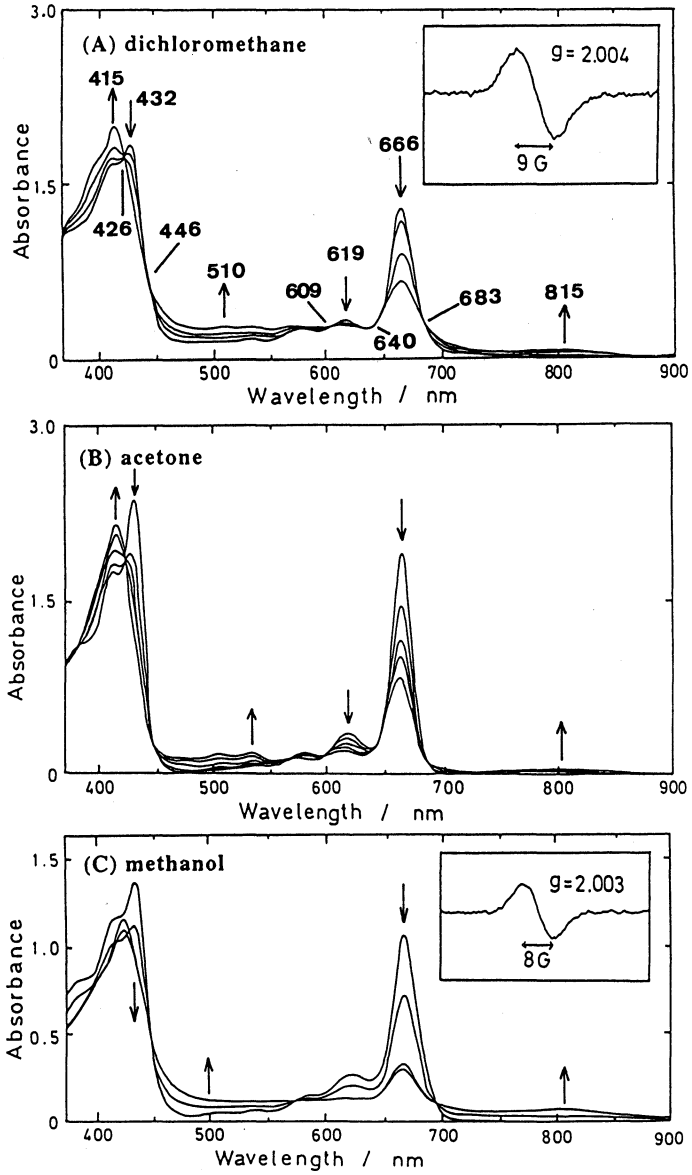

Fig. 2. Absorption spectral changes of Chl with oxidation in (A) CH_2Cl_2, (B) acetone and (C) methanol solutions. The insert figures in (A) and (C) show ESR spectra of $Chl^{+\cdot}$ at a final stage of electrolysis at 0.85 V.

Similar results were also obtained for the other organic solvents such as acetone (Fig. 2 (B), methanol (Fig. 2 (C)), tetrahydrofuran (THF) and acetonitrile. Therefore, it can be concluded that π-cation radical of Chl ($Chl^{+\cdot}$) is efficiently produced via one-electron oxidation of Chl.

Fluorescence spectroscopy of Chl and $Chl^{+\cdot}$

Typical fluorescence spectra of neutral Chl and $Chl^{+\cdot}$ excited at 415 nm are shown in Fig. 3. The fluorescence peak of neutral Chl excited at 415 nm is located at 674 nm for CH_2Cl_2 (Fig. 3 (A)) and at 677 nm for methanol (Fig. 3 (B)). The fluorescence peak of $Chl^{+\cdot}$ formed by oxidation of Chl for CH_2Cl_2 system shifted to 676 nm, while that for methanol system exhibited a blue-shift by *ca.* 6 nm.

A typical fluorescence decay curve of $Chl^{+\cdot}$ for the emission at 680 nm upon excitation at 415 nm is shown in Fig. 4 for acetone system. The decay curve shows a single-exponential decay with a lifetime of 8.5 ns. The lifetime of neutral Chl in acetone solution has been reported to be 6.5 ns (9). The lifetime of $Chl^{+\cdot}$ is longer than that of Chl, suggesting the electronic stability of the excited $Chl^{+\cdot}$ in acetone solution. In this study, we first reported the lifetimes of the excited $Chl^{+\cdot}$ in organic solvents.

Raman spectroscopy of Chl and $Chl^{+\cdot}$

RR spectra of neutral Chl in various organic solvents have been measured to clarify the states of Chl, *e. g.*, axial-coordinate states, self-aggregation and hydrogen bonding between carbonyl oxygen atom and solvent molecule (10-14). The Raman bands in the region of 1750-1000 cm^{-1} for neutral Chl have been assigned to as follows (10, 15): bands in the higher frequency region (1750-1650 cm^{-1}) can be assigned to the keto-carbonyl stretching ($C_9=O$), those in the 1630-1520 cm^{-1} region can be related to both central 16-membered-ring vibrations and C_aC_m or C_bC_b stretching, and those in the region of 1500-1000 cm^{-1} can be assigned to C_aC_m, C_mC_{10} and C_aN stretching modes.

It is expected that the RR spectral changes that occur with oxidation of Chl may show a significant effect on the magnitude of the observed band shifts because of the lower symmetry of Chl. Thus, we measured the RR spectra of $Chl^{+\cdot}$ formed by oxidation of Chl in organic solvents. For all solvents investigated here, oxidation of Chl resulted in a number of RR spectral changes and almost similar

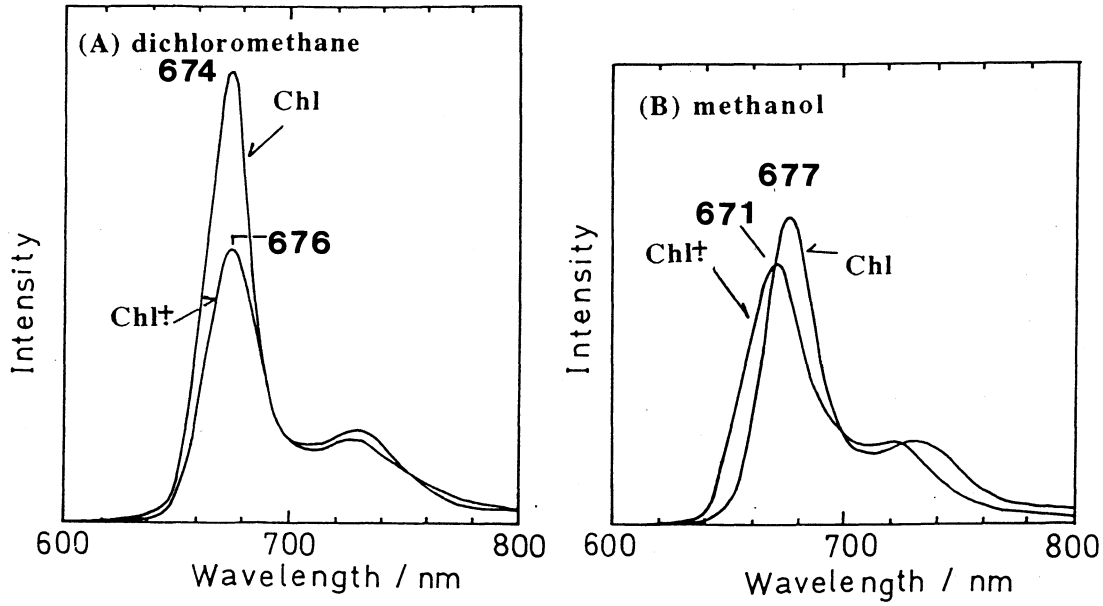

Fig. 3. Fluorescence of spectra of Chl and $Chl^{+\cdot}$ in (A) CH_2Cl_2 and (B) methanol solvent systems. Excitation wavelength: 415 nm.

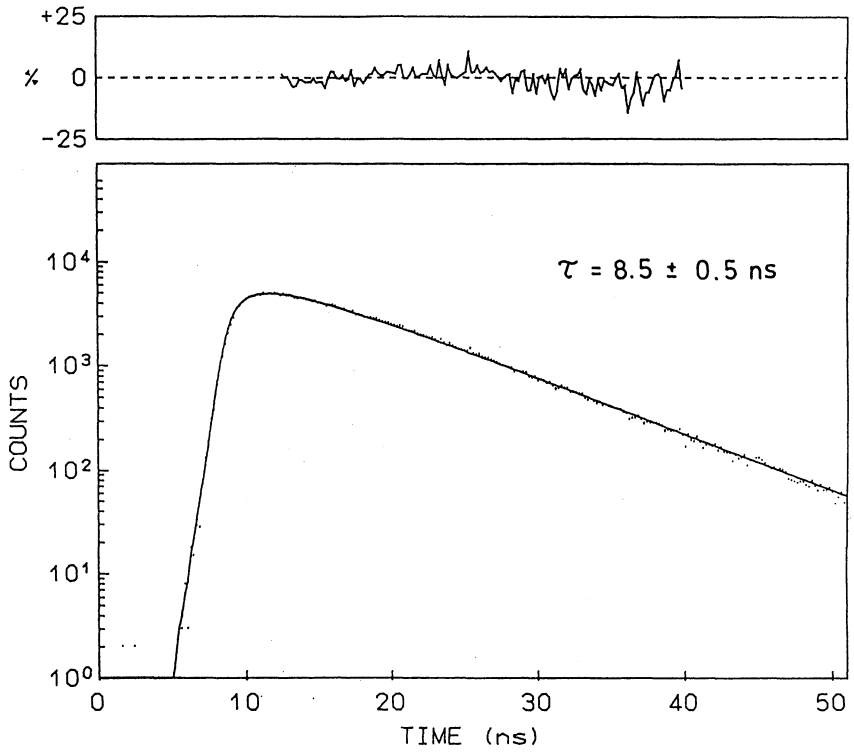

Fig. 4. A fluorescence decay curve of $Chl^{+\cdot}$ in acetone solution. Excitation wavelength : 415 nm. Monitored wavelength : 680 nm.

spectral behaviors were obtained except for THF system. In this section, therefore, we present typical RR spectra obtained from CH_2Cl_2 and THF solvent systems, as shown in Figs. 5 and 6.

For CH_2Cl_2 system in Fig. 5, a Raman band at 1695 cm^{-1} (neutral Chl) assignable to the C_9 keto-carbonyl stretching ($C_9=O$) mode is strongly affected with oxidation and shows a frequency upshift by 15 cm^{-1}. Peaks at 1612 and 1189 cm^{-1} observed for Chl are downshifted to 1596 and 1184 cm^{-1}, respectively. In addition, loss of intensity is observed for bands at 1532, 1337, 1293, 1189 and 1051 cm^{-1}.

As can be seen from Fig. 6, the RR spectra of $Chl^{+\cdot}$ obtained from THF solution were more strongly affected than those from CH_2Cl_2. A Raman band at 1695 cm^{-1} observed for Chl is upshifted to 1710 cm^{-1} with oxidation. It can be seen that there are apparent frequency downshifts of 1596 → 1579, 1180 → 1175 and 1344 → 1332 cm^{-1} with oxidation, while the frequency upshifts of 1546 → 1551 and 1289 → 1293 cm^{-1} are also observed. Moreover, Fig. 6 shows that a significant decrease in intensity is observed for bands at 1520, 1430, 1344, 1289, 1260, 1180 and 1045 cm^{-1} and new bands appear at 1486, 1455, 1230, 1065 and 1032 cm^{-1}. For the purpose of the identification for the prominent RR bands obtained in this work, the frequencies and assignments for CH_2Cl_2 and THF solvent systems are summarized in Table 1.

RR bands at 1695 (CH_2Cl_2) and 1690 cm^{-1} (THF) observed for neutral Chl were the most strongly affected and showed upshifts in frequency by 15-25 cm^{-1} with oxidation. These bands are assigned to the $C_9=O$ stretching mode (10, 15). Heald and Cotton (7) have measured RR spectra of pyrochlorophyll a cation radical in CH_2Cl_2 solution and reported that oxidation of this pigment to form the cation radical results in a decrease in intensity of 1681-cm^{-1} band and the appearance of a new band at 1708 cm^{-1}. This behavior is very similar to that observed for $Chl^{+\cdot}$ in this work. Thus, this fact suggests that the origin of the Raman bands at 1710 (CH_2Cl_2) and 1715 cm^{-1} (THF) observed for $Chl^{+\cdot}$ is

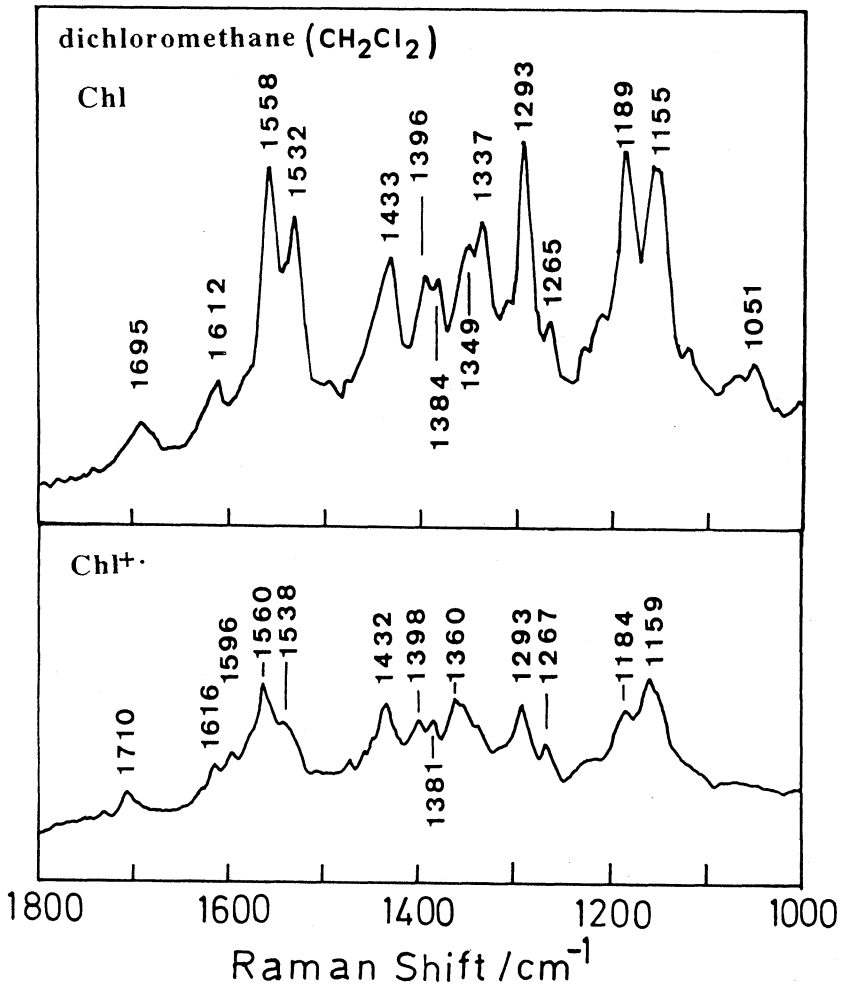

Fig. 5. Resonance Raman spectra of Chl (top) and $Chl^{+\cdot}$ (bottom) in CH_2Cl_2 solvent system.

not the ester group but the C_9 keto group. The large band shift observed for the $C_9=O$ stretching mode may reflect a localization of the major electron density charges at the isocyclic ring. It can be concluded that $Chl^{+\cdot}$ must be in the keto form and not the enol form.

The Raman bands at 1612, 1558 and 1532 cm^{-1} (CH_2Cl_2) and 1596, 1546 and 1520 cm^{-1} (THF) for Chl are known to be sensitive to the coordination-state of Chl and are assigned to C_aC_m or C_bC_b mode (10, 12, 13). A frequency downshift from 1612 to 1596 cm^{-1} and the loss of intensity at 1532 cm^{-1} which may accompany the frequency upshift by 6 cm^{-1} indicate that oxidation of Chl results in reduced electron density on the methine bridge of macrocycle.

In the region of 1500 - 1200 cm^{-1}, the 1337 - and 1293-cm^{-1} bands for Chl in CH_2Cl_2 solution, which are assigned to the C_aN stretching mode, exhibit a decrease in intensity. A new Raman band at 1360 cm^{-1} appears in this solvent; this band can be tentatively assigned to the C_aC_b mode. On the contrary, in the case of THF system, the different spectral behaviors could be observed. Loss of intensity is observed at 1430 (C_aC_m) and 1326 cm^{-1} (C_aN) and the frequency of the 1344-cm^{-1} band (C_aN) is downshifted to 1332 cm^{-1} with Chl oxidation. These results suggest that oxidation of Chl induces the change of substantial spin density at the C_a position of methine carbons of $Chl^{+\cdot}$, resulting in the changes of the C_aC_m and C_aC_b mode bands as well as bands with C_aN mode.

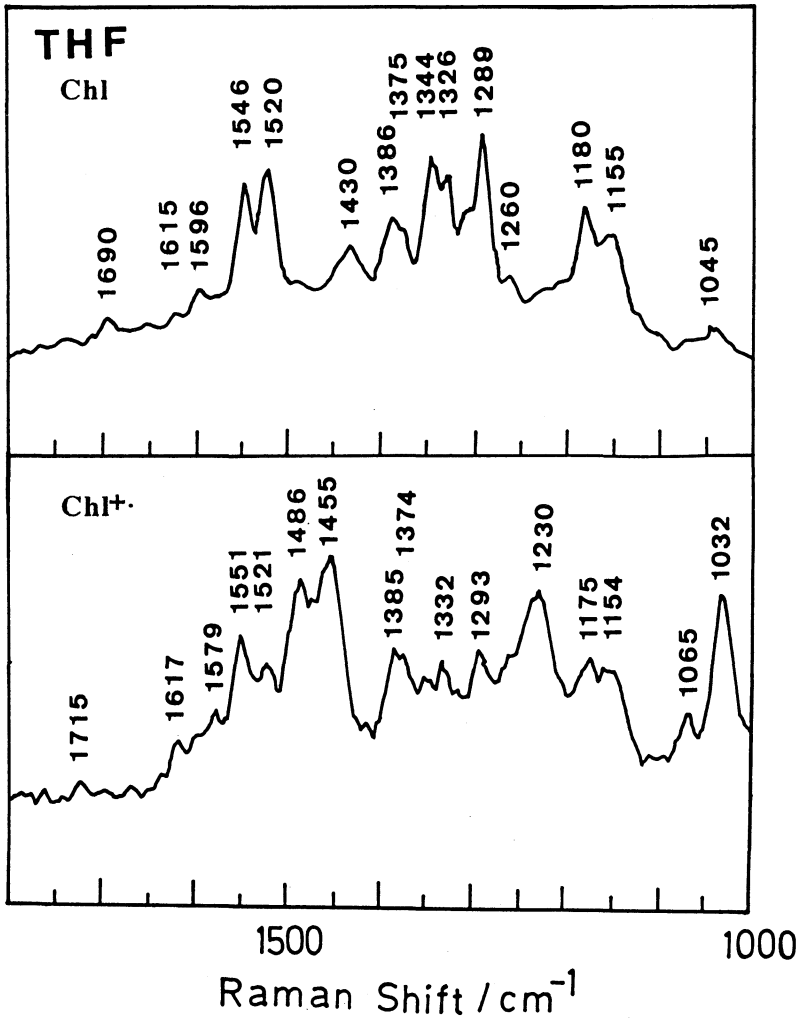

Fig. 6. Resonance Raman spectra of Chl (top) and $Chl^{+\cdot}$ (bottom) in THF solvent system.

In the 1200 - 1000 cm^{-1} region, 1189- (CH_2Cl_2) and 1180-cm^{-1} (THF) bands observed for Chl are, respectively, downshifted to 1184 and 1175 cm^{-1} and also exhibit a decrease in intensity with oxidation. Although the Raman spectrum of neutral Chl in this region usually contains predominantly C_aN modes according to mormal mode assignments (10, 15), Boldt et al. (15) have assigned one band in this region to the C_mC_{10} stretching and reported that this band at 1190 cm^{-1} shifts to 1185 cm^{-1}. The 1184- and 1175- cm^{-1} bands observed in this work, therfore, reflect a change in the electron density within the isocyclic ring with oxidation. In addition, the 1051- (CH_2Cl_2) and 1045-cm^{-1} (THF) bands (C_aN mode) of Chl diappear, while in the case of THF system new Raman bands at 1065 and 1032 cm^{-1} appear upon oxidation; the former band is tentatively assigned to the C_aC_m stretching and the latter one is assigned to the $C_mC_aC_b$ vibration. This difference in two solvent systems may be ascribed to the difference of the coordination-state of Chl; a THF solvent molecule can bind to the central Mg atom of Chl as the fifth-ligand but in the case of CH_2Cl_2 solvent system the coordination number of Chl is four. Thus, the plane-deformation of Chl for THF system may be more strongly induced with oxidation.

Judging from the RR results described above, it can be concluded that oxidation of Chl results in the formation of $Chl^{+\cdot}$ and induces siginificant changes

Table 1. Frequencies (cm^{-1}) of the prominent Raman bands of Chl and $Chl^{+\cdot}$ in CH_2Cl_2 and THF solvent systems

CH_2Cl_2		THF		
Chl	$Chl^{+\cdot}$	Chl	$Chl^{+\cdot}$	Assignment
1695	1710	1690	1715	$C_9=O$
	1616	1615	1617	C_aC_m
1612	1596	1596	1579	C_aC_m
1558	1560	1546	1551	C_bC_b
1532	1538	1520	1521	C_bC_b
			1486	C_aC_m
			1455	CH_3
1433	1432	1430		
1396	1398	1386	1385	C_aN, C_aC_b
1384	1381	1375	1374	C_aC_b
	1360			C_aC_b
1349	1348	1344	1332	C_aN
1337	1338	1326		C_aN
1293	1293	1289	1293	C_aN
1265	1267	1260		C_aN
1189	1184	1180	1175	C_mC_{10}
1155	1159	1155	1154	C_aN, $C_aC_mC_a$
			1065	C_aC_m
1051		1045		C_aN
			1032	$C_mC_aC_b$

in the electron density at the $C_9=O$ bond and in the electron spin density of the macrocyclic π - system. In this study we could observe some $Chl^{+\cdot}$-state marker Raman bands in all organic solvents investigated and conclude that Chl may undergo significant conformational changes with loss of an electron from the C_9 keto-carbonyl group. Finally, the RR results suggest that the $C_9=O$ group of Chl plays an important role in electron transfer in PS I and PS II through its interaction with the proteins.

References

1. M. Y. Okamura, G. Feher and N. Nelson, "Energy Conversion by Plants and Bacteria", Ed. by Govindjee, Academic Press, New York (1982), Vol. 1, P.197.
2. H. J. D. Blanken and A. Hoff, *J. Biochim. Biophys. Acta*, **724**, 52 (1983).
3. J. Fajer, D. C. Borg, A. Forman, D. Dolphin and R. H. Felton, *J. Am. Chem. Soc.*, **92**, 3451 (1970).
4. M. S. Davis, A. Forman and J. Fajer, *Proc. Natl. Acad. Sci. U. S. A.*, **76**, 4170 (1979).

5. J. D. Petke, G. M. Maggiora, L. L. Shipman and R. E. Christoffersen, *Photochem. Photobiol.*, **31**, 243 (1980).
6. R. L. Heald. P. M. Callahan and T. M. Cotton, *J. Phys. Chem.*, **92**, 4820 (1988).
7. R. L. Heald and T. M. Cotton, *J. Phys. Chem.*, **94**, 3968 (1990).
8. J. -H. Perng and D. F. Bocian, *J. Phys. Chem.*, **96**, 10234 (1992).
9. A. Agostiano, K. A. Butcher, M. S. Showell, A. J. Gotch and F. K. Fong, *Chem. Phys. Lett.*, **137**, 37, (1987).
10. M. Lutz, "Advances in Infrared and Raman Spectroscopy", Ed. by R. J. H. Clark and R. E. Hester, Wiely, New York (1984), Vol. 11, P.211; *J. Raman Spectry.*, **2**, 497 (1974); *Biochim. Biophys. Acta*, **460**, 408 (1977).
11. T. M. Cotton and R. P. Van Duyne, *J. Am. Chem. Soc.*, **103**, 6020 (1981).
12. M. Fujiwara and M. Tasumi, *J. Phys. Chem.*, **90**, 250 (1986).
13. M. Tasumi and M. Fujiwara, "Spectroscopy of Inorganic-based Materials", Ed. by R. J. H. Clark and R. E. Hester, Wiley, New York, (1987), Chap. 6.
14. J. Kurawaki and Y. Kusumoto, *Chem. Phys. Lett.*, **158**, 495 (1989).
15. N. J. Boldt, R. J. Donohoe, R. R. Birge and D. F. Bocian, *J. Am. Chem. Soc.*, **109**, 2284 (1987).